Proceedings of 2nd International Sym. Therapeutic Ultrasound
(Seattle, WA, July 29-Aug. 1, 2002)
Ed. by M. A. Andrew, L. A. Crum, and S. Vaezy,
Center for Industrial & Medical Ultrasound,
Applied Physics Laboratory, University of Washington, 2003
pp. 384-390.

Theoretical Results For New Cylindrical Ultrasound Phased Array For Prostate Treatment

Leon A. Frizzell, Joseph S. Tan and Gary M. Warren

Bioacoustics Research Laboratory, Department of Electrical and Computer Engineering, University of Illinois, 405 N. Mathews Ave., Urbana, IL 61801

Abstract. Several groups have examined the design of ultrasound phased arrays for transrectal treatment of the prostate. An effective design must utilize the entire aperture of the array and maintain relatively low grating lobe intensities, ideally while minimizing the number of elements and associated phasing circuitry. In this continuation of our studies to design an array that meets these requirements we examined theoretically a new approach to the design of a cylindrical array. Previous designs have subdivided the cylindrical aperture into several columns of elements oriented along the array length, each with the same center-to-center spacing between adjacent elements. Columns of elements are paired, with the same phasing applied to each of the two corresponding elements within a pair, due to symmetry that applies when focus formation and scanning are limited to a plane bisecting the array in the lengthwise direction. Here we report the results obtained for a novel array where the center-to-center spacing is different for different column pairs. This results in a different location for the grating lobes associated with each column pair, which then no longer reinforce each other. When performance was examined by determining the ratio of the peak focal intensity relative to the maximum intensity of unwanted lobes, G, this array design performed much better than previous designs that we have examined. It was possible to achieve values for G that stayed above 7 when steering the focus 15 mm in either depth or lengthwise directions from its unsteered location.

INTRODUCTION

Two diseases of the prostate, benign prostatic hyperplasia (BPH) and prostate cancer (PC), increasingly afflict our aging male population. Benign prostatic hyperplasia is a nonmalignant enlargement of the prostate that may result in difficulty and discomfort during urination. Fifty percent of all men over the age of 55 suffer from prostate enlargement, and histological evidence of BPH is found in almost all men if they live long enough [1]. Due to its prevalence, treatment costs for BPH represent a substantial portion of the total health expenditures in many countries [2].

Occurrence of prostatic cancer is second to skin cancer in men. It is also the second leading cause of cancer death in American men. In the year 2002, it is estimated that there will be 189,000 new cases and 30,200 deaths due to prostate cancer. Current treatment options include surgery, drugs, and radiotherapy. These treatments can be fairly expensive and are associated with a high incidence of impotence and urinary incontinence, as well as the risks associated with surgical procedures [3]. Since none

of these treatment options are ideal, alternative therapies are currently being sought [2,3].

In recent years, there has been a rise in interest in the use of high intensity focused ultrasound (HIFU) for thermal therapy of the prostate [4,5]. It can produce well-defined regions of thermal necrosis within tissue when applied in a minimally invasive manner, without damaging surrounding and overlying tissue. Local prostate cancer can be controlled with low morbidity, and symptomatic relief of BPH can be provided. It has been shown that HIFU does not enhance metastatic spread of cancer, avoids damage to the rectal wall, and treatment can be repeated for recurrent cancers, unlike radiotherapy.

In the treatment of prostatic disease, ultrasound is applied transrectally. This approach minimizes intervening tissue, which allows the use of higher frequencies with a larger absorption coefficient and more efficient heating of the treatment region. Transrectal treatment limits the size of the acoustic aperture that can be used, but the aperture has been shown to be adequate [4,5]. The thermal sink provided by the cooled coupling fluid surrounding the transducer provides protection for the rectal wall.

Current devices used for HIFU treatment of the prostate use a spherically curved transducer with a fixed focal length. With these systems the focal region is scanned to treat a large volume of tissue by mechanical movement of the transducer. While this mechanical scanning has worked quite successfully [4,5], it is necessary to replace the transducer with one of a different focal length in order to vary the treatment depth.

Several groups have investigated the use of phased arrays to decrease the reliance on mechanical scanning of the transducer, reduce the overall treatment time, and eliminate the need to change transducers. Whereas for some HIFU applications sparsely filled arrays of random distributed elements can be used to decrease grating lobe intensities [6,7], that approach is not possible for transrectal probes as virtually the entire aperture must be used. Thus, other approaches have been examined. For example, it has been shown that the peak intensity of unwanted grating lobes in the field could be decreased by random placement of elements with two different widths within the array [8]. This randomization of element sizes interrupts the regular center-to-center spacing between elements, which significantly decreases constructive interference outside of the intended focal region. However, this approach makes array fabrication more difficult and results in output impedance mismatches between elements, which need to be taken into account.

Previously we examined the effect of array geometry on performance. Studies were conducted on spherical segment, cylindrical, and curved cylindrical arrays to determine their ability to steer in depth and along the length of the prostate [9]. In this study we continue our investigation of the design of phased array transducers that will provide steering in both depth and along the length of the prostate. The goal is to design an array that will provide an acceptable acoustic field, with grating lobes that are acceptably low intensity, while minimizing the number of elements in the array. Herein we report a new approach to decreasing the grating lobes while maintaining a reasonable number of elements.

ARRAY CONFIGURATION

The phased array configuration examined in this study was a cylindrical array which was chosen on the basis of simplicity of design (and therefore ease of manufacture) and superior performance when steered in the y direction (see Fig. 1). The focus of the array was scanned in two dimensions, along the prostate (or y direction) and in depth (or the z direction). It is well known that for such an array grating lobes occur primarily at intervals along the y direction and that their positions are directly dependent upon the center-to-center spacing of the transducer elements. The angular position of the first (strongest) grating lobe in the far field of a one-dimensional linear array is given by the inverse sine of the ratio λ/d, where λ is the wavelength and d is the center-to-center spacing of the elements. The actual angular location of the first grating lobe associated with a cylindrical array is slightly different from that for the linear array, but shows a similar dependence upon d and good agreement for $d/\lambda > 3$.

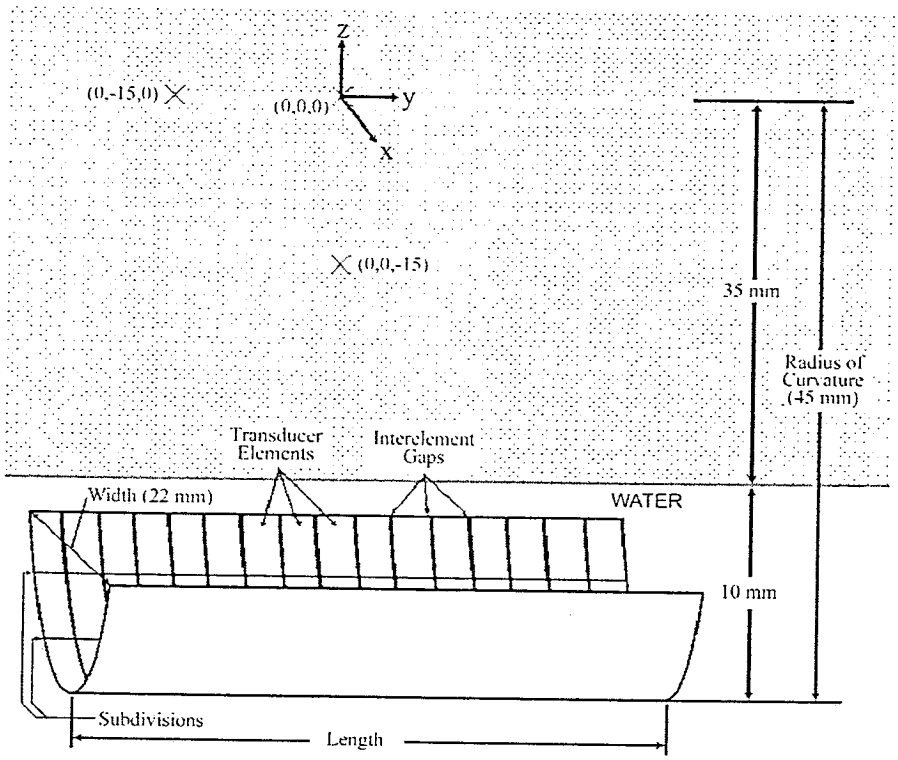

FIGURE 1. Diagram of cylindrical transrectal HIFU applicator, water standoff, tissue, and relevant coordinates.

In order to obtain reasonable grating lobe levels when steering a cylindrical array in the z direction it is necessary to divide the array into several columns of elements [9,10]. These columns are symmetric about a line bisecting the array along its length.

Thus, the array columns can be defined as pairs such that corresponding elements within the pair will each have the same phase for steering and may be connected in parallel to minimize the number of electrical lines in the cable and associated amplifiers. The configuration examined in this study employed a different center-to-center spacing of the elements (a different element width) for each column pair, as shown in Fig. 2. Each element width for this multiwidth cylindrical array applied to a pair of columns symmetrically positioned relative to the y axis, e.g. columns 2A and 2B in Fig. 2. Therefore, each of the paired columns generated grating lobes at different locations in the field. Thus, the array could be designed so that grating lobes produced by different column pairs did not overlap spatially, while the steered foci of each pair of columns still interfered constructively. Note that the column width was adjusted to maintain a constant surface area for all elements and therefore each element exhibits approximately the same impedance.

METHODS

Pressure fields were calculated using the point radiator method [11], which divides the active surface area of the elements into subelements each small enough (one tenth of a wavelength) to produce an acoustic field approximating that of a point source. The total pressure at a given point in the field was calculated as the sum of the complex pressures contributed by each subelement, taking into account the relative phase of the signal applied to the transducer element to which the subelement belongs. Thus the total acoustic pressure at the point (x, y, z) is given by

$$p(x,y,z) \equiv j\frac{\rho c k U_0 \Delta A}{2\pi} \sum_{\text{array surface}} \frac{e^{-[\alpha_W R_W + \alpha_T R_T + jk(R_W + R_T)]}}{R_{Tot}} \qquad (1)$$

where the summation is over the entire active surface of the array, ρ is the density and c is the speed of sound of the medium (taken as 1,000 kg/m^3 and 1,500 m/s, respectively, for both water and tissue), k is the acoustic propagation constant (from $k=2\pi/\lambda$, where λ is the wavelength), U_0 is the velocity amplitude of the surface of the source (calculated from $U_0=(2I_0/\rho c)^{1/2}$, where I_0 = 10,000 W/m^2), ΔA is the area of the subelement, α_W is the attenuation coefficient in water (taken as zero), R_W is the distance that the beam traveled through water, α_T is the attenuation coefficient in tissue (taken as 32.24m^{-1}), R_T is the distance that the beam traveled through tissue, and $R_{Tot} = R_W + R_T$ is the total distance that the beam traveled along the straight line from the source subelement to the field point. All simulations were carried out at a frequency of 4 MHz and the spacing between elements was maintained as half a wavelength.

For a given array configuration, the pressure field was calculated for the focus steered to the anticipated extremes of the treatment region, -15 mm in the y (lengthwise) or z (depth) directions, as well as at the geometric center of the array, 45 mm from the array surface which was defined as the origin of the coordinate system, see Fig. 1. Array performance was assessed by first calculating the acoustic

intensity at each field point, using the equation $I = p^2/2\rho c$, and then finding G, the ratio of intensity at the focus, I_{focus}, to the intensity of the largest unwanted lobe, $I_{max,unwanted}$.

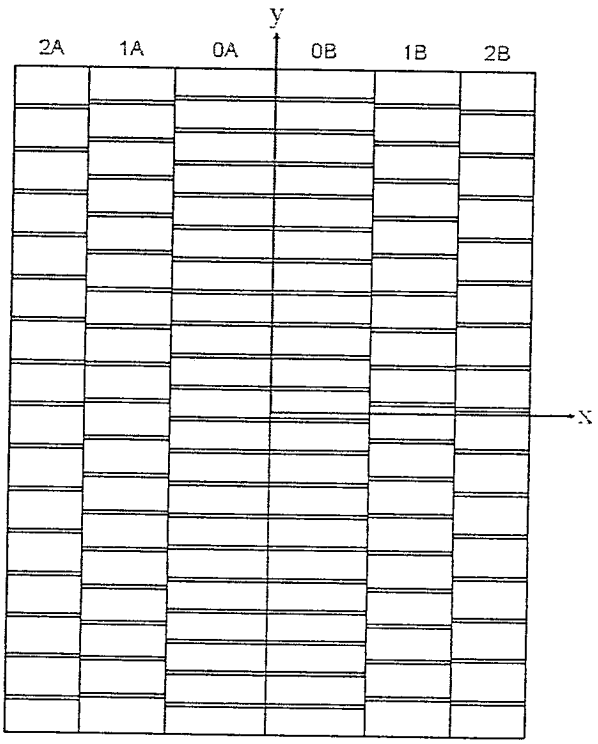

Figure 2. Front face of multiwidth cylindrical transrectal HIFU applicator.

RESULTS

The calculated intensity profile in the y-z plane is shown for two cylindrical transducers with six columns of elements (three column pairs) steered to (0,0,-15) mm, in Fig. 3. The left panel of Figure 3 shows results for an array with a common element width for all columns. This differs significantly from the field shown in the right panel calculated for a multiwidth array (different element width for each of the three column pairs) with the same number of total element pairs. Note that, in contrast to the left panel, the three non-overlapping sets of grating lobes in the right panel have intensities that are very small relative to the focal intensity, and thus are barely visible on the linear scale used.

The performance of several different multiwidth arrays was evaluated by determining the value of G when they were focused at the three positions shown in Fig. 1. The lengths of the arrays examined were 40, 50, and 60 mm, and the number of column pairs was two, three or four. The results consistently showed better performance by a factor of two to three at all three focal positions. When the total

number of element pairs was only 200 it was possible to obtain G values of at least seven.

The shortest arrays seemed to perform best when comparing G versus the total number of element pairs. However, using a sliding subaperture (i.e., a segment of the total array) of a longer array could provide some significant advantages for steering in the y direction. Arrays with two column pairs generally performed best, on a per element basis, at the two focal positions (0,0,0) and (0,-15,0) mm, whereas the four-column-pair arrays performed best with the focus at (0,0,-15) mm. The three-column-pair array appeared to provide the best overall performance when all steering locations were considered.

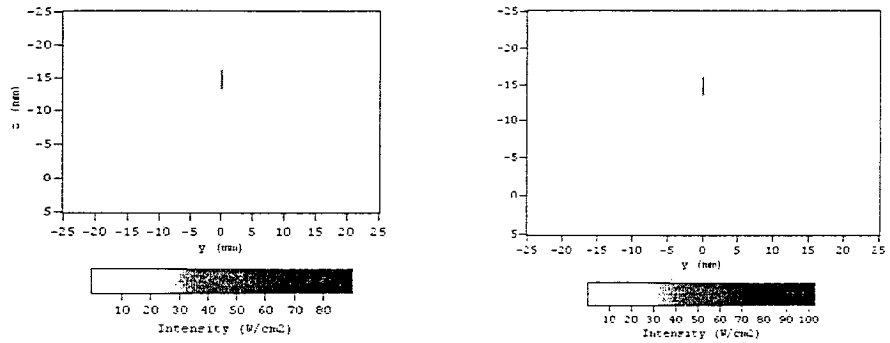

FIGURE 3. Plots of the intensity profile in the z-y plane for a cylindrical array with the same element width for all column pairs (left) and for different element widths (right) for each of the three column pairs.

CONCLUSION

It is apparent that, in all cases, the various multiwidth arrays outperform significantly their single element-width counterparts for a given number of element pairs. The multiwidth array appears to be a promising candidate for HIFU of the prostate.

REFERENCES

1. Grayhack, J.T., Kozlowski, J.M., and Lee, C., *J. Urol.*, **160**, 2375-2380 (1998).
2. De la Rosette, J.M.C.H., D'ancona, F.C.H., and Debruyne, F.M.J., *J. Urol.*, **157**, 430-438 (1997).
3. Parkins, T., *J. Natl. Cancer Inst.*, **86**, 897-898 (1994).
4. Sanghvi, N.T., Foster, R.S., Bihrle, R., Casey, R., Uchida, T., Phillips, M.H., Syrus, J., Zaitsev, A.V., Marich, K.W., and Fry, F.J., *Eur. J. Ultrasound*, **9**, 19-29 (1999).
5. Gelet, A., Chapelon, J.Y., Bouvier, R., Pangaud, C., and Lasne, Y., *J. Urology*, **161**, 156-162 (1999).
6. Frizzell, L.A., Goss, S.A., Kouzmanoff, J.T., and Yang, J.M., *Proc. 1996 IEEE Ultrasonics Sym.*, San Antonio, Texas, Nov. 4-6, 1996, pp. 1319-1323.

7. Goss, S.A., Frizzell, L.A., Kouzmanoff, J.T., Barich, J.M., and Yang, J. M., *IEEE Trans. Ultrason., Ferroelect., Freq. Contr.*, **43**, 1111-1121 (1996).
8. Hutchinson, E.B., Buchanan, M.T., and Hynynen, K., *Med. Phys.*, **23**, 767-776 (1996).
9. Tan, J. S., Frizzell, L. A., Sanghvi, N.T., Seip, R., Wu, J., and Kouzmanoff, J. T., *J. Acoust. Soc. Am.*, **109**, 3055-3064 (2001).
10. Curiel, L., Chavrier, F., Souchon, R., Birer, A. and Chapelon, J. Y., *IEEE Trans. Ultrason., Ferroelect., Freq. Contr.*, **49**, 231-242 (2002).
11. Ocheltree, K.B. and Frizzell, L.A., *IEEE Trans. Ultrason., Ferroelect., Freq. Contr.*, **36**, 242-248 (1989).